the general science journal

Event Horizon Solutions for Rotating Black Holes and a Mechanism for Radio Jets using a Kinematic Spiral Approach

Graeme Heald
16/07/11

Abstract

Event horizons for rotating black holes can be derived in a Euclidean space and absolute time context, not assuming General Relativistic curved space-time. Termed the 'Kinematic Spiral' approach the kinematics of particles attracted to a rotating black hole generates exact solutions for event horizons that are circular or elliptical in plan view and have elongated axial event horizons extending into galactic space for elevational view. A cubic equation is generated with exact solutions for three possible event horizons, with event horizon radii R_C, $R_C^3 = M_\theta \pm \sqrt{(M_\theta^2 - \alpha_\theta^3)}$ where $M_\theta = GM.\sec^2\theta/\omega^2$ and $\alpha_\theta = c^2.\sec^2\theta/3.\omega^2$ for an elevational view. Moreover, axial event horizons offer a possible mechanism for the production of radio jets, acting as funnels for particle ejection from the accretion disk of a rotating black hole. This model corresponds with observations of particle dynamics for rotating black holes.

I. Introduction

In 1963 the Kerr solution found that a spinning black hole would have inner and outer event horizons and an elliptical ergosphere of orbiting particles surrounding the outer event horizon [1-3]. Since that time the hypothesized entity of 'black holes' have been confirmed in an extraordinary variety from supermassive to intermediate and small types usually found within active galactic nuclei and most types are rotating black holes. However, detailed observation has revealed that the Kerr solution does not provide a full description of the real dynamic behaviour of rotating black holes [4-7].

The 'Kinematic Spiral' approach analyses the dynamics of particles captured in the powerful gravitational field of a rotating black hole [8]. By solving the gamma factor singularity, a cubic solution for event horizons is generated, that is the vector sum of the gravitational and rotational velocities squared in terms of the speed of light squared. General Relativistic curved space-time will not be assumed in this approach. This approach also yields the Schwarzschild radius of a 'stellar black hole' if the rotational velocity of the black hole is zero.

Furthermore, the rotation of the black hole about the axis causes the gravitational field to be maximum in the equatorial plane and minimum along the axis of rotation. A plan view of the event horizons in the axis of rotation forms concentric circles and ellipses. When viewed from side elevation from the point of view of particle dynamics, the Kinematic Spiral solution generates event horizons with spikes along the axis of rotation. Polar plots show that event horizons form dual 'teardrop' shaped figures.

Powerful jets of plasma that emerge from black holes termed 'radio jets' can reach thousands of light years in length. However, the radio jet mechanism remains unknown to date, as the observations cannot distinguish between theoretical models. The composition of the jet is hypothesized to be an electrically neutral mixture of protons, positrons and electrons. Radio jets radiate in a wide range of wavebands from radio to the gamma ray spectrums via synchrotron and inverse Compton effect [11-12].

Two competing theories for the mechanism of the radio jets are the 'Blandford-Znajek' and 'Penrose mechanism'. The 'Blandford-Znajek' model [9] asserts that the twisting of magnetic field lines by the accretion disk collimates the outflow along the axis of the central object, so that a radio jet will emerge. The magnetic field lines around the accretion disk are dragged by the spin of the black hole. The accretion disk material launches the radio jets by the tightening of the field lines. The second 'Penrose mechanism', extracts energy from the rotating black hole by frame dragging. Axial holes in the event horizons have also been suggested as a mechanism for radio jets [7]. This theory demonstrates an ability to extract particle energy from the accretion disk as a mechanism for the formation of radio jets [10-11].

II. Particles Spiralling into Rotating Event Horizons

i) A Kinematic Approach to Event Horizons

A rotating black hole has maximum rotational energy orthogonal to the axis of rotation and zero rotational energy along the axis of rotation. From the relativistic or proper momentum, L_o, the singularity can be derived:

$L_o = m.v.\delta(t)$

where m, mass of a high speed particle,
v, is the velocity
gamma factor, $\delta = 1/\sqrt{(1 - v(t)^2/c^2)}$

When the velocity of the particle tends to the speed of light, both the gamma factor and the momentum tend to infinity.

$$\delta = 1/\sqrt{(1 - v(t)^2/c^2)} \quad (1)$$

If $v(t) \rightarrow c$ then $\delta \rightarrow \infty$ and $L_o \rightarrow \infty$

It should be noted that the kinematic approach also provides the correct Schwarzschild radius of a 'stellar black hole' if the rotational velocity of the black hole is zero, $v_{rot} = 0$, with only the gravitational potential and velocity, v_G, extant:

$c = |v_G|$

$c = \sqrt{2GM/R}$

$c^2 = 2GM/R$

$$R = 2GM/c^2 \quad (2)$$

The equation generates a single spherical or elliptical event horizon for the 'stellar black hole' (2).

ii) Kinematic Spiral Solution Plan View

When viewed along the axis of rotation, the event horizon radius, denoted, R_C, for spiralling particles can be calculated from the vector sum of gravitational velocity, v_G, and the rotational velocity, v_{rot}, equated with the speed of light:

$c^2 = |v_G|^2 + |v_{rot}|^2$

$c^2 = 2GM/R + \omega^2.R^2$

$\therefore \omega^2.R^3 - Rc^2 + 2GM = 0$

$$\therefore R^3 - c^2/\omega^2 R + 2GM/\omega^2 = 0 \quad (3)$$

The cubic equation (3) has exact solutions:

$R_C = \sqrt[3]{(GM/\omega^2) + \sqrt{((GM/\omega^2)^2 - (c^6/27\omega^6))}} + \sqrt[3]{(GM/\omega^2) - \sqrt{((GM/\omega^2)^2 - (c^6/27\omega^6))}}$

$$R_C = \sqrt[3]{(GM/\omega^2) \pm \sqrt{((GM/\omega^2)^2 - (c^6/27\omega^6))}} \quad (4)$$

Simplifying let $M_\omega = GM/\omega^2$ and $\alpha = c^2/3\omega^2$

$R_C^3 = M_\omega \pm \sqrt{(M_\omega^2 - \alpha^3)}$

$$R_C = \sqrt[3]{(M_\omega \pm \sqrt{(M_\omega^2 - \alpha^3)}} \quad (5)$$

Where $G = 6.67 \times 10^{-11}$, M is mass of black hole, ω angular speed and $c = 2.998 \times 10^8$ m.s^{-1}.

Equation (5) provides exact solution for a 'plan view' along the axis of rotation of particles spiralling into a rotating black hole. A maximum of three concentric event horizons occur for rotating black holes and these are denoted R_{C1}, R_{C2}, and R_{C3} respectively, please see figure 1. The size of the event horizon radii in plan view has been shown to closely correspond with event horizons of observed rotating black holes [8-9].

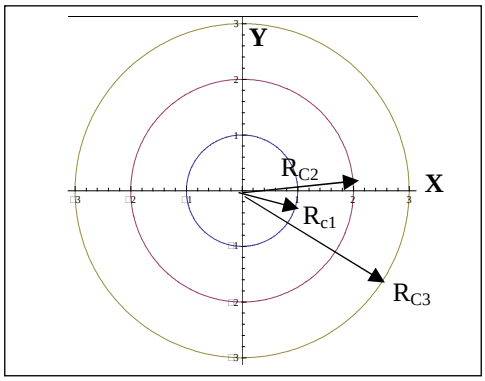

Figure 1. Plan View of Circular Kinematic Spiral Event Horizons

iii) Kinematic Spiral Elevational Solution

The angular velocity of particles motion in a gravitational field diminishes to zero on the axis of rotation and is maximal in the ecliptic plane of the rotating black hole. Where θ is the angle aligned to the axis of rotation, the angular velocity is given by:

$v = \omega.R.\cos\theta$

In this case the X and Y axis are fixed at 0° and 180° and the axes of rotation are at 90° and 270° as shown in figure 3. The orthogonal view to the axis of rotation the event horizon radius denoted, R_C, for spiralling particles can be calculated from the vector sum of gravitational velocity, v_G, and the rotational velocity, v_{rot}, equated with the speed of light:

$c^2 = |v_G|^2 + |v_{rot}|^2$

$c^2 = 2GM/R + \omega^2.R^2.\cos^2\theta$

$\therefore \omega^2.R^3.\cos^2\theta - Rc^2 + 2GM = 0$

$\therefore R^3 - R.c^2/(\omega^2\cos^2\theta) + 2GM/(\omega^2.\cos^2\theta) = 0$ (6)

The cubic equation (6) has exact solutions:

$R_C = \sqrt[3]{(GM.\sec^2\theta/\omega^2) \pm \sqrt{((GM\sec^2\theta/\omega^2)^2 - (\sec^2\theta c^6/27\omega^6))}}$ (7)

Simplifying let $M_\theta = GM.\sec^2\theta/\omega^2$ and $\alpha_\theta = c^2.\sec^2\theta/3.\omega^2$

$R_C^3 = M_\theta \pm \sqrt{(M_\theta^2 - \alpha_\theta^3)}$

$R_C = \sqrt[3]{(M_\theta \pm \sqrt{(M_\theta^2 - \alpha_\theta^3)}}$ (8)

Equation (8) provides exact solutions for a side elevation view of particles spiralling into a rotating black hole along the axis of rotation. A maximum of three event horizons occur for rotating black holes and these are denoted R_{C1}, R_{C2}, and R_{C3} respectively. A three-dimensional triple event horizon structure is formed that is concentric when viewed from above and extends along the axis of rotation when viewed from side elevation. This solution has precedence in the 'Onion skin' model of active galactic nuclei [6]. Consisting of orbiting plasma particles and light the phenomenon of the black hole ‘accretion disk’ [4] occurs at 0° and 180° in side elevation along the X and Y axis.

III. Simulations of Kinematic Spiral Solution

i) Two Dimensional Plots of Event Horizons

Event horizons for rotating black holes of various values of period and mass will be demonstrated in figures 2 to 6. Where $M_\theta = GM.\sec^2\theta/\omega^2$ and $\alpha_\theta=c^2.\sec^2\theta/3.\omega^2$ plots of M_θ and α_θ have been given for different relationships. In figures 2 to 6 the accretion disk would be located along the x-y axis at the origin, where the rotational and gravitational field of the rotating black hole is strongest. However, it should be noted that the anticipated circular or elliptical shaped black hole is not confined to the origin.

The different shapes of the event horizon or radio jets, whether thin or wide at the origin, is dependent upon the scaling relationship between M_θ and α. Figures 3 and 4 show axial event horizons converging at a distance from the black hole for $M_\theta >> \alpha$. Figures 3 to 6 for $M_\theta > \alpha$, $M_\theta = \alpha$ and $M_\theta < \alpha$ provide event horizons that begin wide at the black hole and converge slowly at a distance from the black hole.

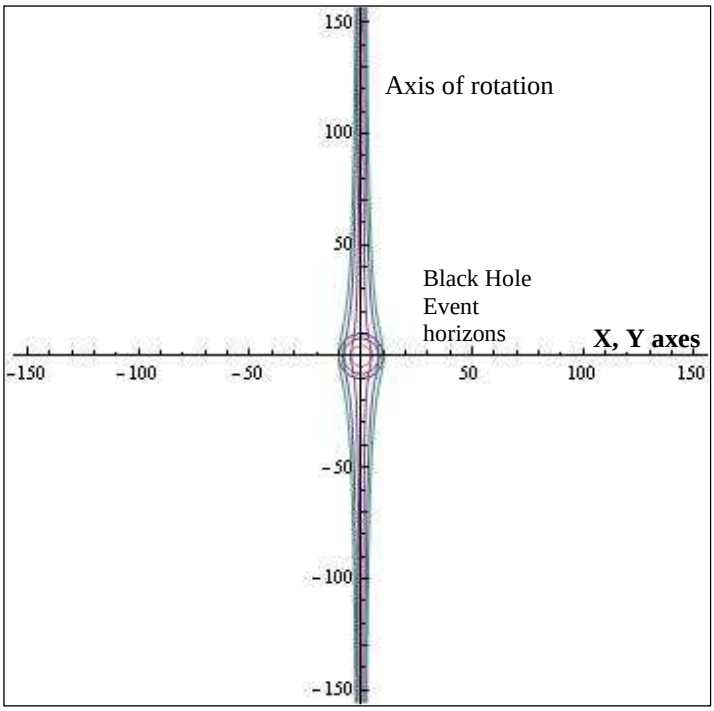

Figure 2. Side Elevation View of 3 Kinematic Spiral Event Horizons, $M_\theta > 0$ and $\alpha_\theta = 0$.

In figure 2 the values used in the plot are: $M_{\theta 1} = 1000.\sec^2\theta$, $M_{\theta 2} = 500.\sec^2\theta$, $M_{\theta 3} = 500.\sec^2\theta$ and $\alpha_{\theta 1} = \alpha_{\theta 2} = \alpha_{\theta 3} = 0$.

Figure 3 represents the generic case for rotating black holes when the rotational mass, M_θ, is much greater than the alpha factor, that is, $M_\theta >> \alpha_\theta$.

Figure 4 represents the generic case for rotating black holes when the rotational mass, M_θ, is greater than the alpha factor, that is, $M_\theta >> \alpha_\theta$. The values used in the plot are: $M_{\theta 1}=1000.\sec^2\theta$, $M_{\theta 2}=2000.\sec^2\theta$, $M_{\theta 3}=3000.\sec^2\theta$, $\alpha_{\theta_1}=10\sec^2\theta$, $\alpha_{\theta_2}=20\sec^2\theta$, $\alpha_{\theta_3}=30\sec^2\theta$. This represents the generic case when the rotational mass, M_θ, is greater than the alpha factor, α_θ, that is, $M_\theta > \alpha_\theta$.

Figure 5 represents the generic case when the rotational mass, M_θ, is equal to the alpha factor, α_θ, that is, $\alpha_\theta = M_\theta$.

The values in Figure 6 used in the plot are: $M_{\theta 1} = 100.\sec^2\theta$, $M_{\theta 2}=200.\sec^2\theta$, $M_{\theta 3}=300.\sec^2\theta$, $\alpha_{\theta_1}=100\sec^2\theta$, $\alpha_{\theta_2}=200\sec^2\theta$, $\alpha_{\theta_3}= 300\sec^2\theta$.

Figure 6 represents the generic case when the rotational mass, M_θ, is less than the alpha factor, α_θ, that is, $\alpha_\theta > M_\theta$. The values in Figure 6 are: $M_\theta = 10.\sec^2\theta$, $\alpha_{\theta_1}=1000.\sec^2\theta$.

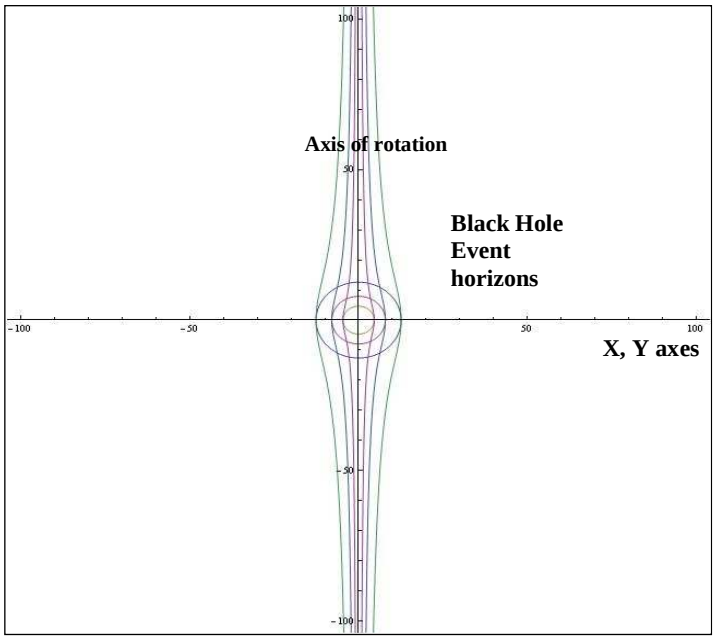

Figure 3. Side Elevation view of 3 Kinematic Spiral Event Horizons, $M_\theta >> \alpha$.

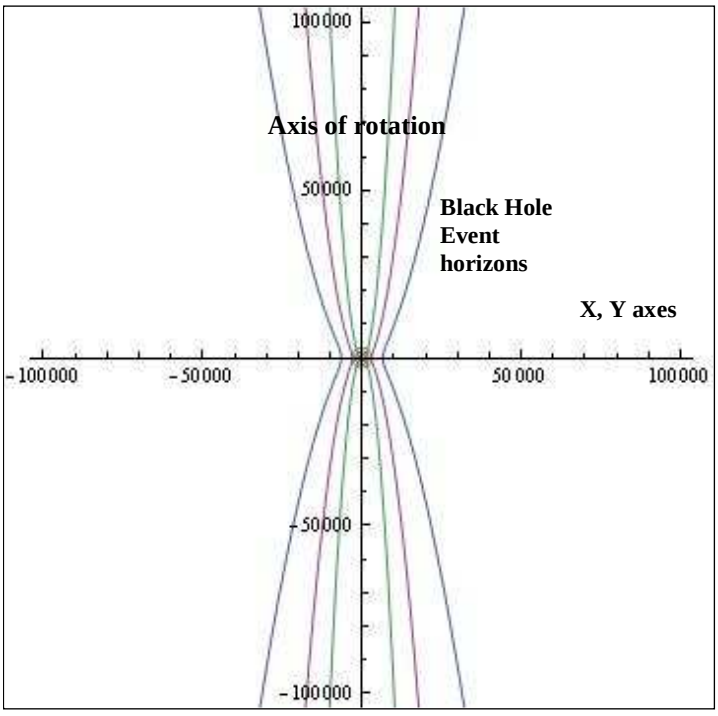

Figure 4. Side Elevation View of 3 Kinematic Spiral Event Horizons, $M_\theta > \alpha_\theta$.

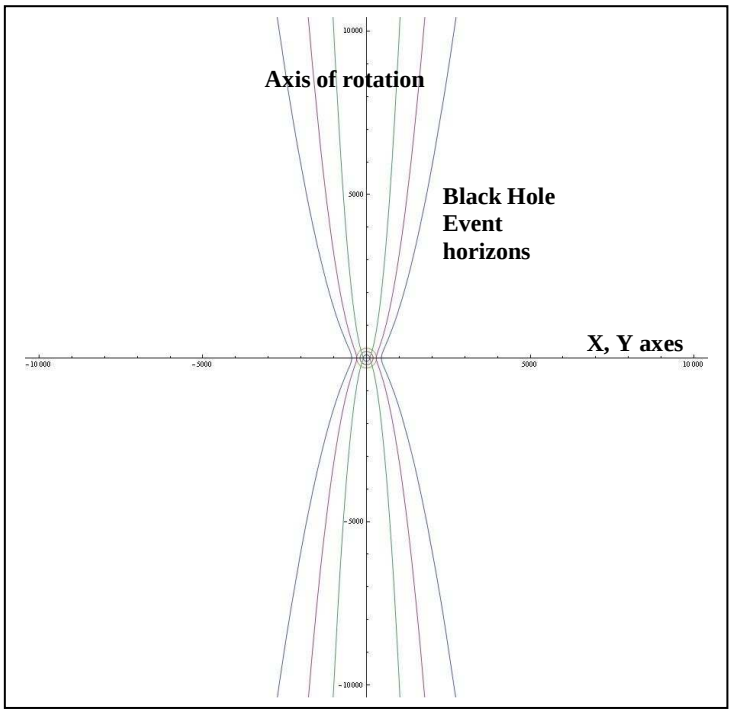

Figure 5. Side Elevation View of 3 Kinematic Spiral Event Horizons, $M_\theta = \alpha_\theta$.

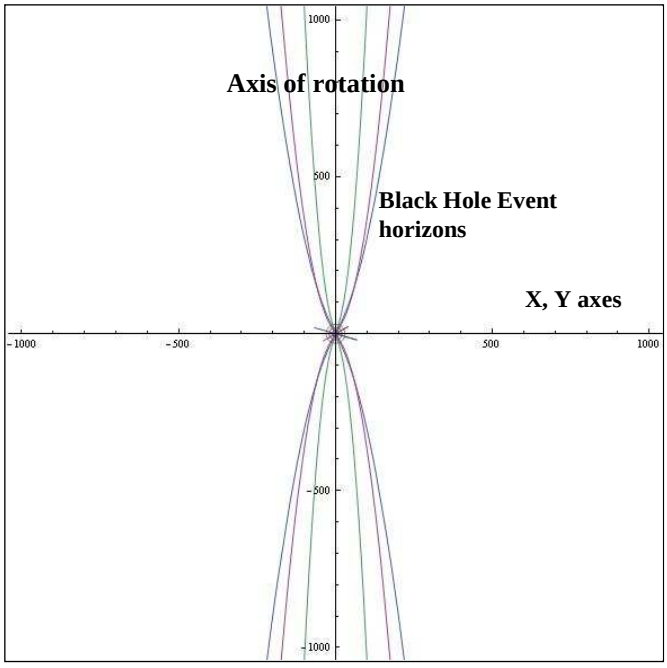

Figure 6. Side Elevation View of 3 Kinematic Spiral Event Horizons, $\alpha > M_\theta$

IV. On Radio Jets

Initially plasma particles would be attracted to the strong rotational gravitational field of a black hole. This dynamic would cause an accretion disk of high-speed plasma to orbit around the central event horizon. Orbiting plasma particles could be dislodged by instabilities induced by high electrical and magnetic fields. High-speed particles could then be ejected from the accretion disk and travel in helical trajectories away from the black hole as shown in figure 7. The elevational solutions for axial event horizons, suggests that particles can be ejected along the axial event horizons as radio jets.

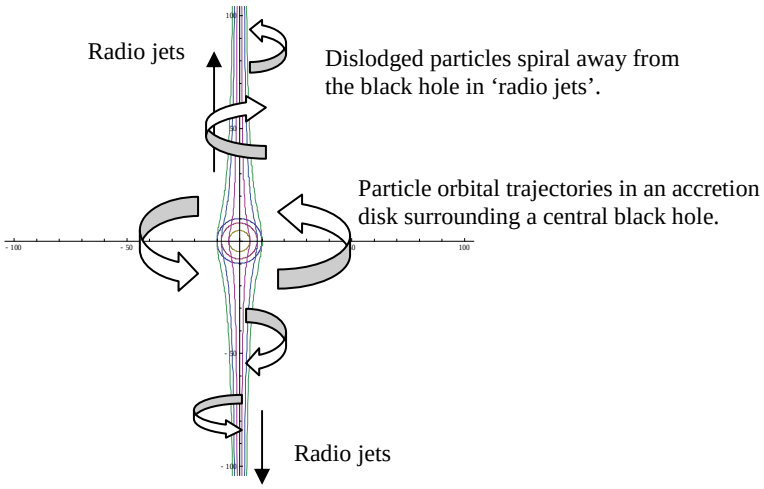

Figure 7. Side Elevation View showing Radio Jets produced by Kinematic Spiral Event Horizons

To overcome the attraction of powerful gravitational field towards the rotating black hole, the particles need to have high energy with speeds close to the speed of the light. The event horizons converge into straight lines at a distance from a black hole as shown in figure 7. The ejected plasma stream would then be collimated, as observed from a distance and, without gravitational obstruction travel great galactic distances prior to dispersion.

The plasma travels along magnetic field lines induced by the accretion disk according to the Blandford-Znajek model for radio jets. It is of note that the magnetic field lines induced from an electrical current outside a solenoid, or coil, forms a continuous torus shape running to the opposite magnetic poles along the axis. The accretion disk with rotating charged particles would then induce continuous torus shaped field lines along the axis of the rotating black hole up to the event horizon. However, observation reveals that the plasma jets are constrained to well-defined hollow helical orbits as they travel from the black hole, as shown in figure 9. Furthermore, the radiation is continuous and broad spectrum from the radio to the x-ray regions in most radio jets. Hence, this model cannot be fully correct.

The Kinematic Spiral event horizon provides for collimation of the plasma beam away from the black hole. Evidence for this viewpoint is provided in figure 8, for example the high-resolution radio-wavelength image of the source of the jet in galaxy M87 near a black hole. The inset images present a large scale view, while the main picture shows a high-resolution image of the jet much closer to the black hole. (Courtesy, NRAO)

The trajectory of particles has been observed to be helical within light days of the black hole [13]. As the plasma travels further away from the black hole in 'Centaurus A' radio images for example, reveal a variety of internal knots, rings, loops and filaments and helix threads [14]. The ejected plasma in radio jets travels around axial event horizons demonstrated in figures 2 to 6, while the relationship between M_θ and α_θ shapes the axial horizons.

An artist's impression of the radio jet emission from a black hole reported by: Junor et al., in *Nature*, 28 October 1999, is given in figure 9. This represents a typical model of the Blandford-Znajek model showing particles ejected in helical trajectories along magnetic field lines. Astronomical research, however, better supports the Kinematic Spiral model. The following images of black holes demonstrate this finding as radio jets can be clearly observed in the article entitled "Origin of M87 Jet Near a Black Hole".

V. Images of Black Holes and Radio Jets

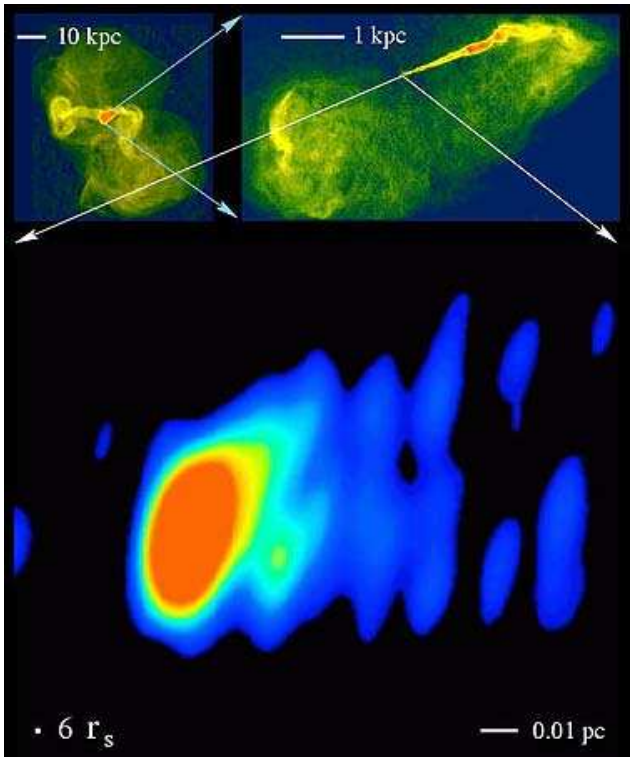

Figure 8. Source of the Jet in Galaxy M87 near a presumed Black Hole

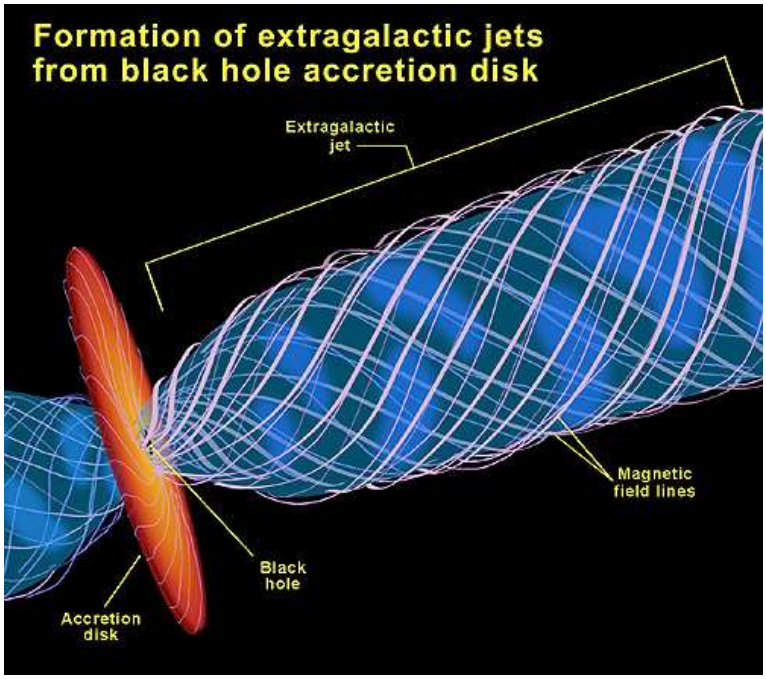

Figure 9. A model of a jet, shaped by strong, twisting field lines, blasts upwards from the accretion disk around the black hole. (Courtesy, Space Telescope Science Institute.)

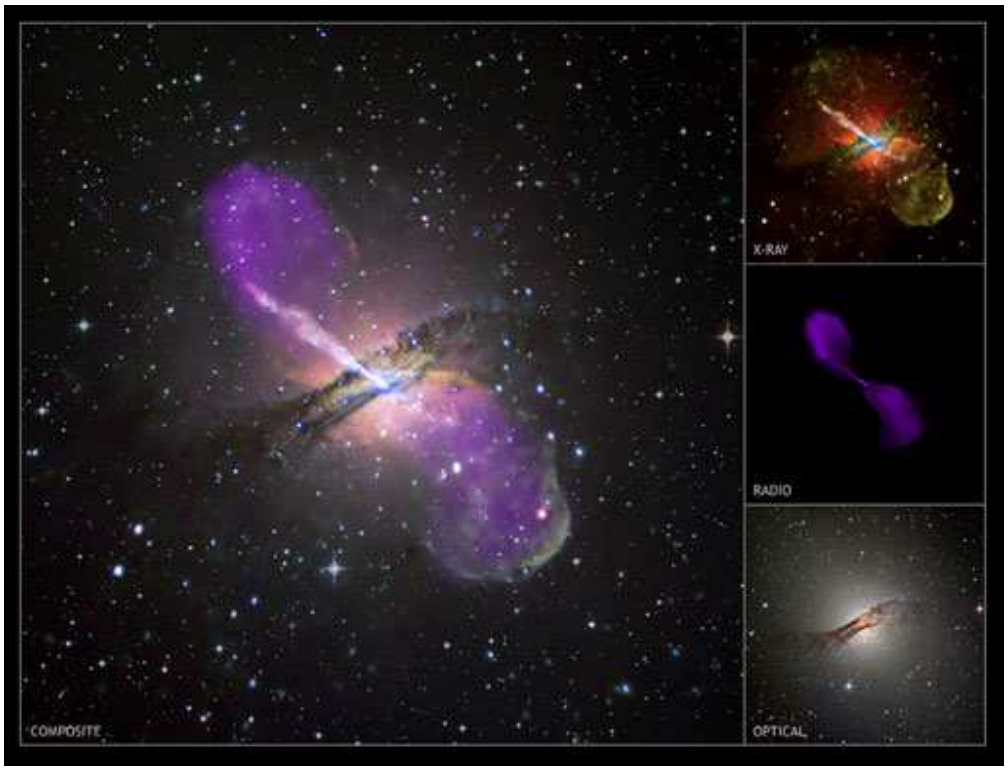

Figure 10. Composite Image of the Centaurus A, Supermassive Black Hole showing Radio Jets

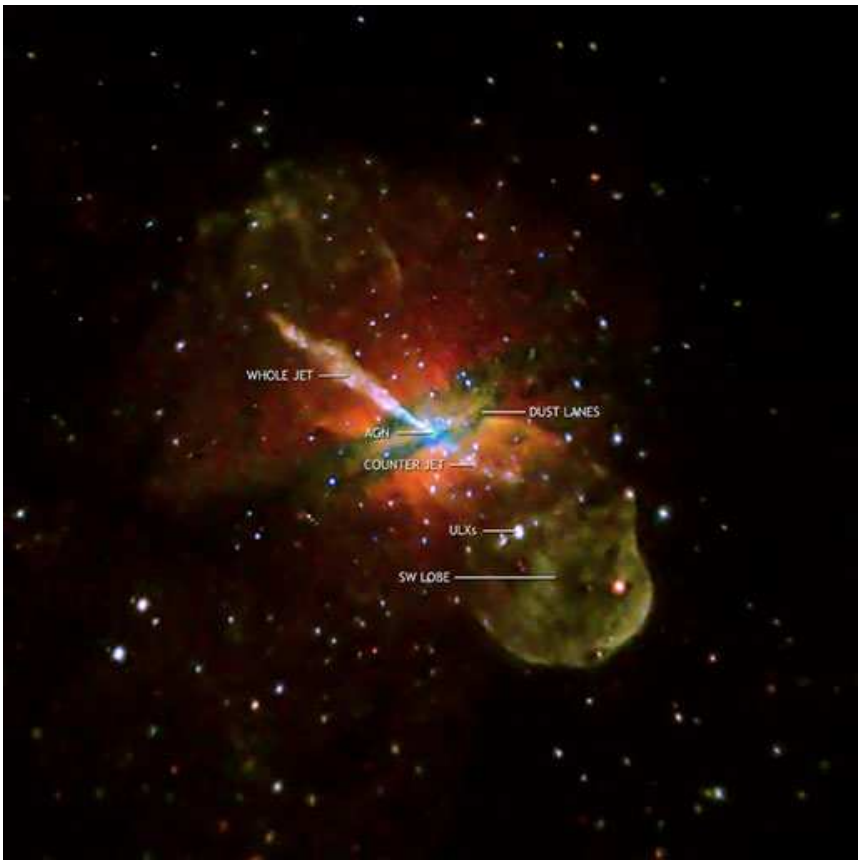

Figure 11. Important features of the Centaurus A Black Hole

Figure 10 Image Credit: X-ray: NASA/CXC/CfA/R.Kraft et al; Radio: NSF/VLA/Univ.Hertfordshire/M.Hardcastle; Optical: ESO/VLT/ISAAC/M.Rejkuba et al. This shows a composite of an image as seen from the x-ray, radio and optical images of the Chandra telescope trained on event horizons and radio jets from Centaurus A supermassive black hole. Opposing jets of high-energy particles can be seen extending to the outer reaches of the galaxy, and numerous smaller black holes, in binary star systems, are also visible. Reference: "*Jet power and black hole assortment*", http://spacespin.org/article.php/80123-jet-power-black-hole-assortment#, dated Jan 9, 2008.

Figure 11 Image Credit: NASA/CXC/CfA/R.Kraft et al. This labeled image highlights some of the important features of the Chandra X-ray Observatory image of Centaurus A. The active nucleus and the launching point for a jet are featured at the center of the galaxy. Particles in the jet, and radiation from the active nucleus, are both powered by a supermassive black hole. The jet is shown to the upper left, and the shorter "counterjet" points in the opposite direction. Reference:"*Jet power and black hole assortment*", http://spacespin.org/article.php/80123-jet-power-black-hole-assortment#, dated Jan 9, 2008.

The composite image for the rotating black hole in the nucleus of Centaurus A in figure 10 demonstrates the 'dusty cyclone' accretion disk and the radio jet phenomenon in the visible, x-ray and radio wavelengths. In particular, the cross sectional view looking towards a black hole corresponds with the elevational view of the Kinematic Spiral event horizons in figure 11. Further resemblance is shown to the observations of supermassive black holes NGC 6166, NGC 4278, NGC 4374 M84 [15], M87 supermassive black hole [16-17], and Sagittarius A*; the supermassive black hole at the centre of the Milky Way galaxy [18].

Particle ejection from strong gravitational fields of black holes can be explained in terms of the extended axial event horizons and the unstable orbits of high-energy particles in the accretion disk. Axial event horizons form funnels that divert unstable particles away from the black hole central event horizon in a spiral trajectory. The helical trajectory about the axial event horizons causes a continuous and broad spectrum of radiation in the ejected plasma.

VI. Conclusion

This paper has shown that event horizons for rotating black holes can be derived in a Euclidean space and absolute time context. The 'Kinematic Spiral' approach offers an exact cubic solution of event horizons, as an alternative to the Kerr solution. As given in equation (8) the event horizon radii R_C in elevational view for angle θ:

$$\mathbf{R_C = \sqrt[3]{M_\theta \pm \sqrt{(M_\theta^2 - \alpha_\theta^3)}}}$$

Where $G = 6.67 \times 10^{-11}$, M is mass of black hole, ω is angular speed and $c = 2.998 \times 10^8$ m.s^{-1}
and $M_\theta = GM.\sec^2\theta/\omega^2$ and $\alpha_\theta = c^2.\sec^2\theta/3.\omega^2$

As given in equation (5) in plan view, $\theta = 0°$:

$$\mathbf{R_C = \sqrt[3]{(M_\omega \pm \sqrt{(M_\omega^2 - \alpha^3)}}}$$

where $M_\omega = GM/\omega^2$ and $\alpha = c^2/3\omega^2$

In plan view the radii of event horizons agrees with observations of black hole event horizons [8]. In side elevation, the solutions form extended axial event horizons into galactic space. Combining the plan and elevation views, the Kinematic Spiral generates dual 'teardrop' and wide angle shaped event horizons as observed in the complex dynamical behaviour of rotating black holes.

As alternative explanation to the 'Blandford-Znajek' and 'Penrose' mechanisms, the 'Kinematic Spiral' approach offers a plausible model for the formation of radio jets. There appears to be a basis for radio jet formation in the axial event horizons shaped by the equations defining the event horizons for rotating black holes, given above. Thus, the kinematic approach offers a model for the size and number of event horizons; and a mechanism for the formation of radio jets for rotating black holes without the assumption of relativistic curved space-time.

References

[1] Kerr, R.P "Gravitational Field of a Spinning Mass as an example of algebraic Special metrics", Phys. Rev.Lett, 11, 237-238, 1963.
[2] Kerr, R.P "Gravitational Collapse and Rotation", Phys. Rev.Lett, 1964.
[3] D. Wiltshire, "The Kerr Spacetime: Rotating Black Hole in General Relativity", Cambridge Uni Press, UK, 2009.
[4] R.M. Wald, "Black Holes and Relativistic Stars", Uni of Chicago, pp 79-102, 199).
[5] F. Melia, "The Black Hole at the Centre of the Galaxy", Princeton Uni Press, 200).
[6] J.H. Krolik,"Active Galactic Nuclei", Princeton Uni Press, New Jersey, pp 495-496, 1999.
[7] A. Burinskii, E. Elizalde, S.R. Hildebrandt G. Magli, "Rotating ''black holes'' with holes in the horizon", Phys. Rev. D **74,** 021502(R) , 2006.
[8] G. Heald, "Kinematic Spiral Solutions for the Event Horizons of Rotating Black Holes", General Science journal**,** Astrophysics,http://wbabin.net/weuro/heald2.pdf, Sep.2010.
[9] S.S. Doeleman, et al, "Event Horizon scale structure in the supermassive Black Hole candidate at the Galactic Centre", Nature 455, 78-80, 4 Sep 2008.
[10] R.D. Blandford, R.L. Znajek, Monthly Notices of the Royal Astronomical Society, 179, 433, 1977.
[11] R.Penrose "Gravitational Collapse: The role of General Relativity", Nuovo Cimento Rivista, Numero Speciale 1, 252-276, 1969.
[12] R.K.Williams "Extracting x-rays, δ rays and relativistic e+e- paris from supermassive Kerr black holes using the Penrose mechanism", Phys. Rev. 51(10), 5387-5427, May 15, 1995.
[13] Wehrle. A.E, Zacharius. N, Johnston.K, ET AL "What is the Structure of Relativistic Jets in AGNs on Scales of Light Days?", white paper, 11 Feb 2009, http://www.nrao.edu/A2010/whitepapaers/rac/Wehrle_AGN_jets_GCN.pdf
[14] Melia F. "The Edge of Infinity, Supermassive Black Holes in the Universe', Cambridge Uni Press, UK, 2003.
[15] C. Ly, R. C. Walker, and J. M. Wrobel "An attempt to probe the radio jet collimation regions in NGC 4278, NGC 4374 (M84), and NGC 6166", The Astro. Journal, **127**: 119–124, Jan. 2004.
[16] M. A. Dopita, A.P Koratkar, M.G.Allen, Z.I. Tsvetanov, H.C. Ford, G.V.Bicknell, R.S. Sutherland, "The liner nucleus of M87: a shock-excited dissipative accretion disk", The Astro. Journal, **490**:202 E215, November 20, 1997
[17] A.E. Broderick, A.Loeb, "Imaging the black hole silhouette of M87: implications for jet formation and black hole spin." The Astro. Journ., **697**:1164–1179, June 1, 2009.
[18] Melai, F. "The Black Hole at the Centre of the Galaxy", Princeton Uni Press, 2003.